A low-dimensional dynamic model of severe slugging for control design and analysis

Espen Storkaas[†] Sigurd Skogestad[†], and John-Morten Godhavn[‡]

[†]Dep. Of Chemical Engineering, Norwegian University of Science and Technology, N-7491 Trondheim, Norway

[‡]Statoil ASA, R&D, Process control, Arkitekt Ebells vei 10, Rotvoll, N-7005 Trondheim, Norway

ABSTRACT

We have developed a simplified dynamic model of multiphase flow in the type of systems that severe slugging occurs. Inside the open loop slug regime, the model covers both the stable limit cycle known as slug flow, and even more importantly, the unstable but preferred stationary flow regime, making it suitable for controller design.

We have fitted the model to data both from a simulation (OLGA) test case and from medium-scale experiments. We have in both cases achieved good agreement with the data, and controllers designed based on our model are able to stabilize the flow for the systems modeled.

1 INTRODUCTION

Multiphase transport of gas, oil and water has become increasingly important for the offshore oil industry. The trend towards more satellite wells leads to longer multiphase transport pipelines from the well clusters and wellhead platforms into the production platforms. In addition to the increased length, greater depths provide additional challenges for flow assurance.

The flow regime known as slug flow is characterized by intermittent axial distribution of liquid and gas. The bulk of the liquid is transported as slugs, where the pipe flow consists of pure liquid. The gas is transported as bubbles between the liquid slugs. Slug flow can be divided into hydrodynamic and gravity induced slugging (also called terrain induced slugging). Hydrodynamic slugging occurs in near horizontal pipelines and is caused by velocity differences between the phases and will not be treated here.

Gravity induced slug flow are generally induced by a low point in the pipeline topography. A typical situation is that liquid accumulates at a low point at the bottom of the riser, blocks the flow of gas and initiates the slug cycle. The prerequisites for this to occur are relatively low pipeline pressure and flow rates. Gravity induced slugs are often long, and thus associated with severe pressure oscillations.

The flow and pressure oscillations due to gravity induced slugging have several undesirable effects on the downstream processing facilities. They will create severe feed disturbances for the inlet separator, causing poor separation and in some cases overfilling. The oscillations may also affect the compressor trains, resulting in unnecessary flaring. Other adverse consequences are wear and tear on the equipment resulting in possible unplanned process shutdowns.

The severe slugging problem can be solved by increasing the pressure drop over the topside (or wellhead) choke valve. However, the increased pressure drop will lower oil recovery, and is not an optimal economic solution. Other proposed solutions such as installing slug catchers are given in (1).

Using active control to prevent severe slugging has been proposed in (2) and by other researchers. Control based strategies have recently received a lot of attention and are currently viewed as a promising solution. Both implementations and commercial products exist, as reported in (3), (4) and (5). These control systems are designed based on simulations using rigorous multiphase simulators, process knowledge and trial and error.

Using active control to stabilize an unstable operating point has several advantages. Most importantly, one is able to operate with even, non-oscillatory flow at a pressure drop that would otherwise give severe slugging. This will in turn lead to less need for topside equipment, higher production, higher oil recovery and less wear and tear on the equipment.

To design efficient control systems, it is advantageous to have an accurate model of the process. When modeling for control purposes, one should keep the control objective and its associated timescale (bandwidth) in mind. One should only include those physical phenomena that are significant at the relevant timescales in the model, something that allows us to use simpler models for control purposes than for more detailed simulations.

There are two common methods for modeling multiphase flow. The first is called a two-fluid model, where one uses partial differential equations (PDE's) for conservation of mass and momentum in each phase. The other is a drift flux model, where one has PDE's for conservation of mass in each phase, and a combined momentum conservation equation. More details on modeling of multiphase flow can be found in (6) and (7). These PDE-based modeling techniques are versatile, even though empirical correlations are needed, and can be adapted to a wide range of flow regimes.

The drawback of these models from a control point of view is that they are infinite-dimensional, thus poorly suited for conventional control design methods. This can partially be remedied by discretizing in space, but the resulting set of ordinary differential equations (ODE's) will be large. We originally used a PDE based two-fluid model in our work (8), a two fluid model (4 PDE's) discertized with 25 grid points yielding an ODE model with 100 states. This is too many state variables for efficient analysis and controller design. The control objective is to stabilize an unstable operating point, and the relevant timescale is the speed of which the instability evolves. Keeping that in mind, a lot of the spatial variations and fast dynamics included in the PDE based models are unnecessary. This leads us to the conclusion that it should be possible to develop a simpler model that describes the dominant behavior of a system with severe slugging.

2 MODEL DESCRIPTION

To achieve the size and complexity reduction in the model that would be desirable, the basic modeling principles must be changed. We focus on describing the observed macro-scale behavior rather than the detailed physics that governs the flow. Since severe slugging basically is a pressure-gravity driven process, it is natural to try to describe it using bulk terms rather than spatial variables.

The macro scale behavior that we want to describe includes:

- the stability of the solutions and the operational conditions as function of choke valve opening
- the nature of the transition to instability
- the presence of an unstable stationary solution at the same choke valve openings as those corresponding to severe slugging
- the amplitude/frequency of the oscillations

Note that we for control purposes are more interested in the desired (unstable) operating behavior than the open loop (no control) severe slugging behavior. This means that the three first points on the above list of objectives are more important than the last one.

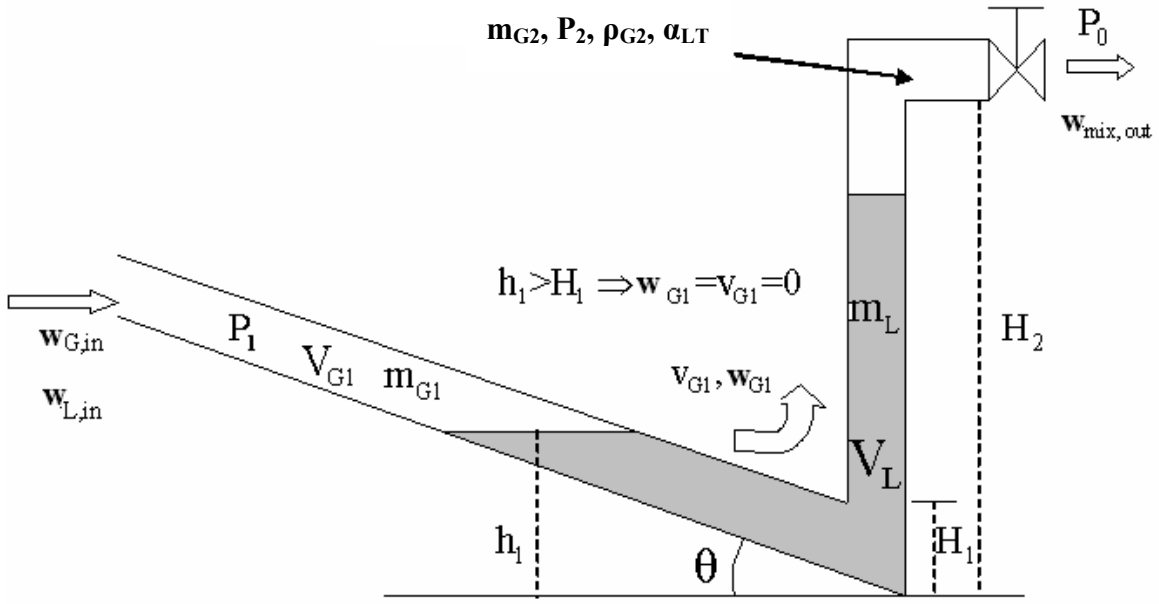

Figure 1: Model characteristics with important parameters

2.1 Assumptions

We will base our modeling on the setup depicted in Figure 1. Our main assumptions are:

- Constant liquid velocity in "feed" pipeline (neglecting liquid level dynamics). This implies:
  - Constant upstream gas volume (volume variations due to liquid level at the low point are neglected)

    - Constant liquid feed directly into riser
- Only one liquid control volume (which includes both riser and part of the feed pipeline)
- Two gas control volumes, separated by the low point, and connected through a pressure-flow relationship.
- Ideal gas behavior
- Stationary pressure balance between riser and feed section
- Simplified choke model for gas and liquid leaving the riser
- Constant system temperature

2.2 Model fundamentals

The model has three states; the holdup of gas in the feed section, the holdup of gas in the riser, and the holdup of liquid. The corresponding mass conservation equations are:

$$\frac{d}{dt}m_L = w_{L,in} - w_{L,out} \quad [1]$$

$$\frac{d}{dt}m_{G1} = w_{G,in} - w_{G1} \quad [2]$$

$$\frac{d}{dt}m_{G2} = w_{G1} - w_{G,out} \quad [3]$$

Based on the description in Figure 1, the computation of most of the system properties such as pressures, densities and phase fractions is straight forward. We use a stationary pressure balance over the riser, where the pressure drop equals the weight of the fluids in the riser. The use of a stationary pressure balance is justified because the pressure dynamics are significantly faster than the time scales in the control problem. For long pipelines, it might be necessary to add some dynamics between the riser-bottom pressure and the measured pressure if the pressure sensor is located far from the riser. The boundary condition at the inlet can either be constant or pressure dependent inflow. We use a simplified valve equation (eq. 4) to describe the choke valve at the outlet.

$$w_{mix,out} = K_1 z \sqrt{\rho_T \left(P_2 - P_0\right)} \quad [4]$$

The crucial part of the model is to describe the distribution and velocities of the two phases in the riser. This is described in detail below. The entire model is given in detail in Appendix A. A Matlab version of the model is available on the web (9).

As it is given above, the model must be solved as a differential-algebraic (DAE) system. However, through a state transformation, it is possible to transform the system into a set of ordinary differential equations (ODE's), which may be necessary in order to perform a range of nonlinear analyses such as Lyapunov based stability calculations. The state transformation is given in Appendix B.

2.2.1 Relationship between gas flow into riser and pressure drop

For the gas phase, neglecting the acceleration terms, the pressure difference $\Delta P = P_1 - P_2$ is the sum of the frictional pressure drop and the static pressure drop.

$$\Delta P = \Delta P_f + \rho_L g h \quad [5]$$

For turbulent flow

$$\Delta P_f = \sum_i c_i \rho_i \frac{v_i^2}{2} \quad [6]$$

Where ΔP_i is the individual frictional pressure drops, and the c_i's are friction coefficients. Focusing on the low point and assuming that the pressure drop is purely frictional, we get

$$\Delta P = \left(P_2 - P_1 - \alpha_L \rho_L g H_2\right) = c \rho_{G1} \frac{v_{G1}^2}{2} \quad [7]$$

Clearly, the friction coefficient c depends on the relative "opening" $(H_1-h_1)/H_1$, and assuming an inverse quadratic dependency gives eq. 8. The corresponding mass flow is given by eq. 9 where $\hat{A}$ is the gas flow area at the low point. Note that combining equations 8 and 9 with $f(h_1)=(\hat{A}(H_1-h_1)/H_1)$ yields a "valve equation" (eq. 10) where the functional dependency on $((H_1-h_1)/H_1)$ is approximately quadratic.

$$v_{G1} = \begin{cases} K_2 \frac{H_1 - h_1}{H_1} \sqrt{\frac{P_1 - P_2 - \rho_L g \alpha_L H_2}{\rho_{G1}}} & \forall\, h_1 < H_1 \\ 0 & \forall\, h_1 \geq H \end{cases} \quad [8]$$

$$w_{G1} = v_{G1} \rho_{G1} \hat{A} \quad [9]$$

$$w_{G1} = K_2 f\left(h_1\right) \sqrt{\rho_{G1}\left(P_1 - P_2\right)} \quad [10]$$

2.2.2 Entrainment equation

The final important element to determine is the fluid distribution in the riser. This can be done in several ways. One is using a slip relation similar to the one used in drift flux modeling to determine the liquid velocity and from that calculate the distribution. Attempts to do this were not successful. Another way is to model the two-phase flow as entrainment of liquid by the gas. We found that this was better (and easier), and we choose to use an entrainment equation relating the fraction of liquid in the top (α_{LT}) to other system variables. The two extreme cases are no entrainment (liquid behaves as if in a tank) and no slip ($\alpha_{LT}=\alpha_L$) for high flow velocities. The transition between them should be smooth, but how steep the transition should be will probably be case dependent. We will consider a transition as depicted in Figure 2, where the parameter q depends on the gas velocity in the system.

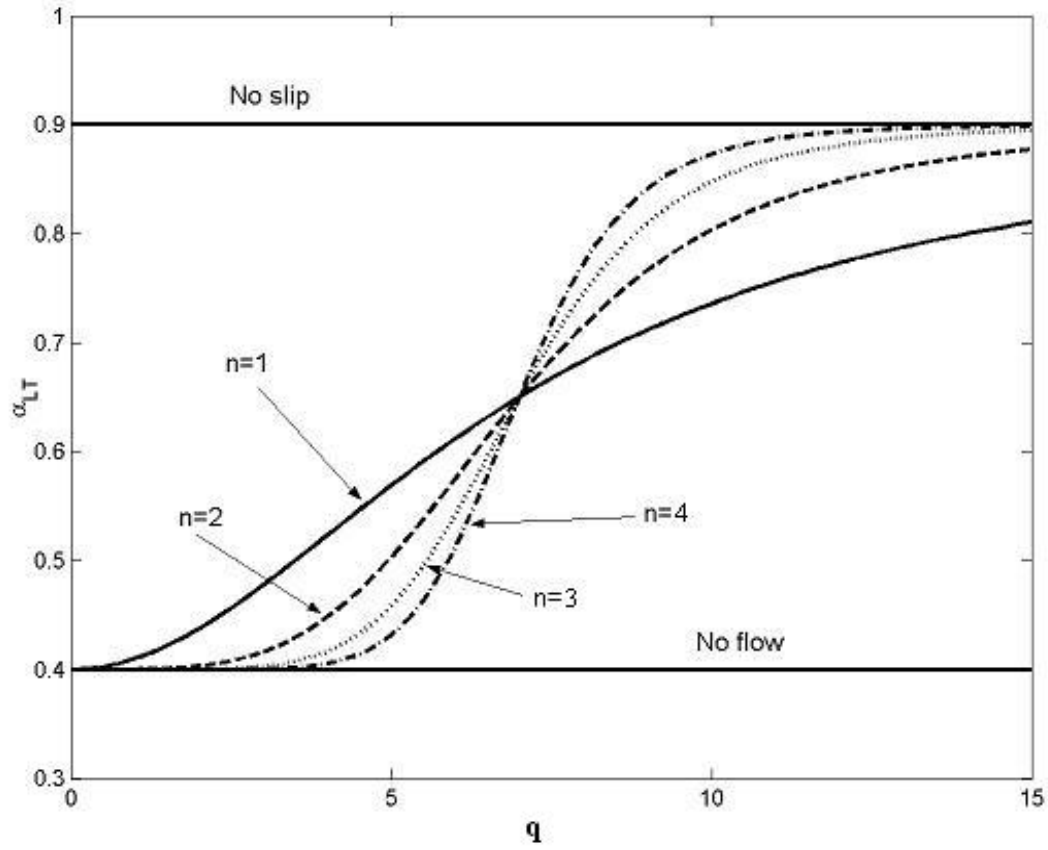

Figure 2: Entrainment with different slopes

The entrainment in slug flow is somewhat similar to flooding in for example distillation columns. The flooding velocity in a distillation column is equal to the terminal velocity for a falling liquid drop and is given by

$$v_f = k\sqrt{\frac{\rho_L - \rho_G}{\rho_G}} \qquad [11]$$

This expression only gives a yes/no answer to whether it is flooding or not. To get a smooth transition, we use the square of the ratio of the internal gas velocity v_{G1} to the flooding velocity as a parameter (eq. 13). The entrainment equation in eq. 12 produces the transition depicted in figure 2, where the parameter n is used to tune the lope of the transition. The parameter K_3 in eq. 13 will shift the transition along the horizontal axis.

$$\alpha_{LT} = \alpha_{LT} + \frac{q^n}{1+q^n}(\alpha_L - \alpha_{LT}) \qquad [12]$$

$$q = k\frac{v_{G1}^2}{v_f^2} = \frac{K_3 \rho_{G1} v_{G1}^2}{\rho_L - \rho_{G1}} \qquad [13]$$

Note that we use the velocity at the low point (v_{G1}) to obtain the entrainment of liquid through the riser. This is because the impulse of the gas at the low point initiates the entrainment by affecting the velocity of the incompressible liquid. By assuming that the average gas impulse responsible for the entrainment of liquid through the riser is linearly dependent on the impulse of gas through the low point, the use of v_{G1} in the entrainment equation is justified.

3 MODEL TUNING

The model parameters K_1, K_2, K_3 and the exponent n in the entrainment equation are free parameters that can be used to tune the model. In addition to these, one can also vary the compressibility in a corrected ideal gas law and the upstream gas volume to achieve better fit to the data. The upstream gas volume can be used because this represents the effective volume available for the gas and will depend on the amount of liquid present in the feed pipeline.

The tuning of the model will depend on the available data. If one has a dependable, detailed model of the system available, one can generate the data needed. If the system is already operational, field data is a better alternative. In this work we have based the tuning on data from the point where the unstable region begins, that is, the highest valve opening with stable operation. Earlier work (8) has shown that the system goes through a Hopf bifurcation at this point. A Hopf bifurcation point is characterized by having a pair of complex imaginary eigenvalues (poles). This information together with two other measurements of, for instance, pressures in the system can be used to initiate the system to steady state. The last of the main tunable parameters (K_1, K_2, K_3 and n) should be found by iterating on the value of h_1 until a satisfactory behavior is achieved, as this has to lie in the interval $0<h_1<H_1$ to ensure consistency. Finally, one can tune the compressibility and the upstream gas volume V_{G1} to get an acceptable fit of pressure levels, amplitudes, and frequencies for other valve openings.

4 CASE 1: COMPARISON TO OLGA DATA

To illustrate the use of the simplified model, we will use data from the test case for severe slugging in OLGA. OLGA is a commercial multiphase simulator widely used in the oil industry. The case geometry is given in Figure 3. It is a constant mass flow with constant liquid fraction into the system. The pressure after the choke valve is constant at 50 Bar.

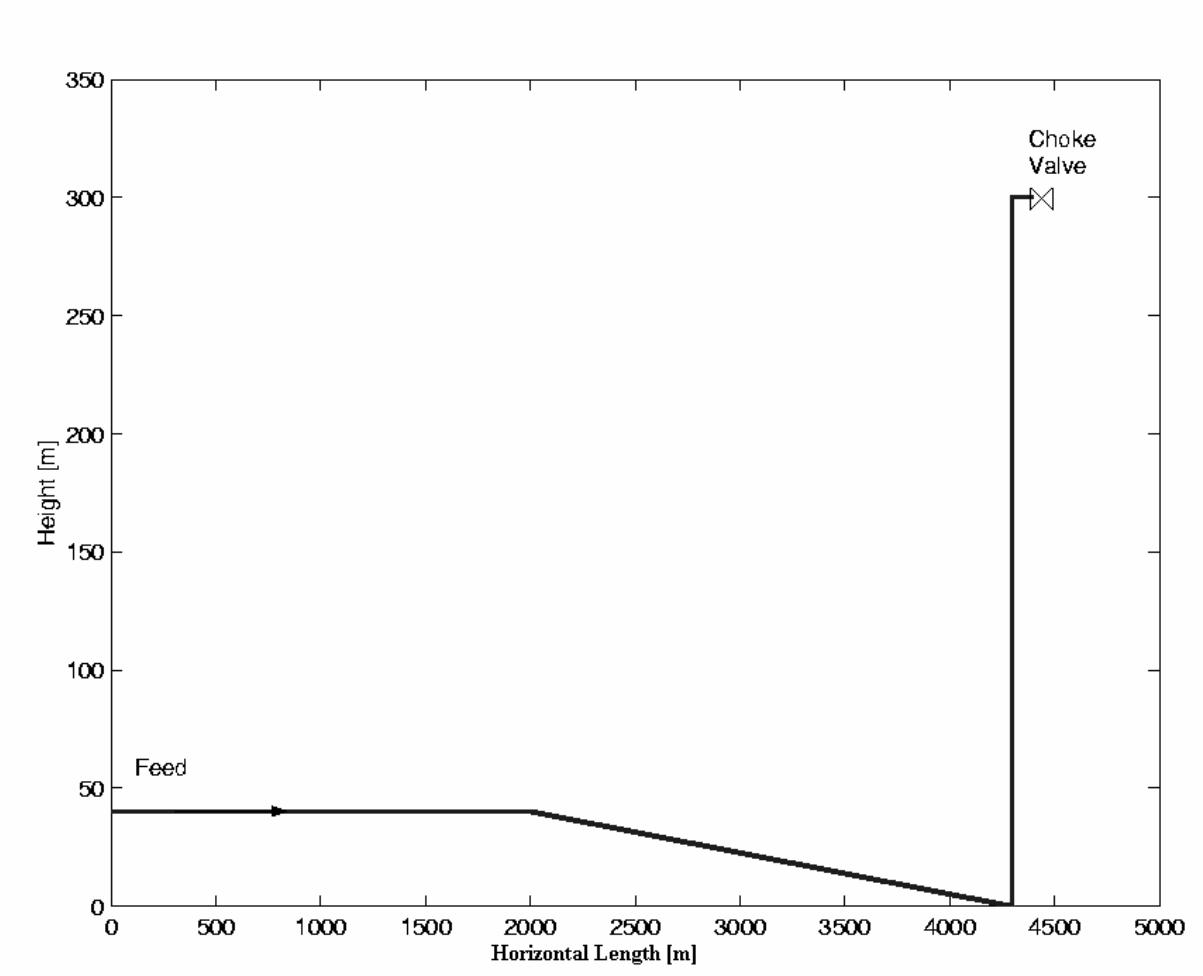

Figure 3: Case 1 geometry

Based on OLGA simulations, a bifurcation diagram for the system was made. The bifurcation diagram is given in Figure 4. The upstream pressure is given on the vertical axis and the valve opening is on the horizontal axis. The bold lines are the results from the OLGA simulations. The bifurcation diagram shows that for valve opening up to 0.13, the system is stable, as indicated by the single bold line. For valve openings over 0.13, we would normally have severe slugging with maximum and minimum pressures given by the solid bold lines. Initiating OLGA to steady state gives the unstable stationary solution indicated by the dashed bold line.

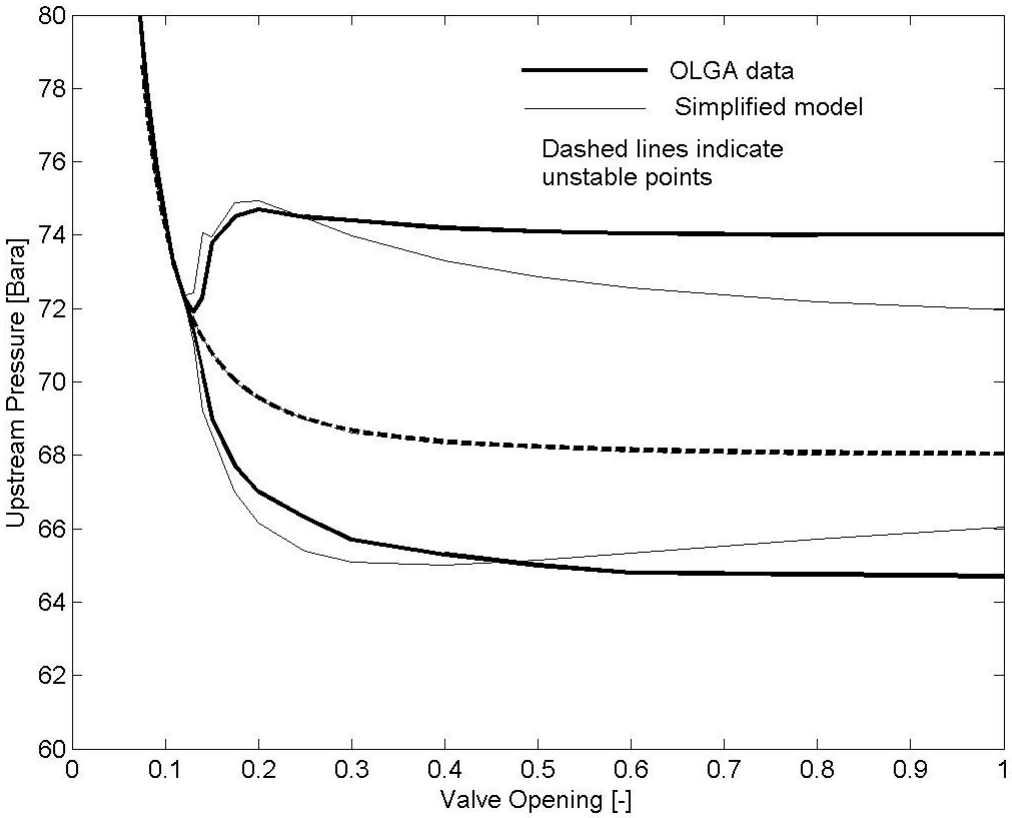

Figure 4: Bifurcation diagram for the case 1

The model was tuned as described above. It is unrealistic to achieve a good fit to both the slug regime and the stationary regime over the entire range of valve openings, so some priorities have to be made. First, the unstable, stationary regime is more important than the stable oscillatory regime. The reason for this is that we wish to avoid the slug regime, and operate at the stationary regime, hence we focus on where we want to be and not on where we don't want to be. A parallel to this can be found in everyday life; if you are teaching someone to ride a bike, you are teaching them how the bike behaves when they have mastered the balancing act (the desired unstable operating point), not how it behaves when it lies on the ground (the undesired slug flow).

Second, we will focus in the low to medium valve openings. The reason for this is that for the controller to work, the control actuator has to have a significant impact on the process. For the high-range valve openings, the pressure drop over the choke valve is too small for the effect of a small change in valve opening to be significant. This means that we can only operate in the low to medium valve opening range. This is really not a restriction, because, as can be seen from the bifurcation chart, there is no significant incentive to operate at higher valve openings. There is an insignificant difference between the upstream pressures for valve openings between 0.4 and 1.

As can be seen from Figure 4, the fit of the simplified model (thin lines) to the reference data from OLGA is good. The fit for the stationary data is excellent, and the fit for the oscillatory data in the low to medium range are also good. The deviations in amplitude at higher valve openings are acceptable in light of the priorities behind the model fitting. The frequency of the oscillations are not included in the bifurcation diagram, but comparisons between the

results show that the slug frequency is about 10-20% higher for the simplified model for low to medium range valve openings and up to about 50% higher for high valve openings. The higher frequency comes from neglecting the liquid dynamics in the feed section. We have in this case tuned to achieve a good fit for the amplitude, and when the upstream gas volume is fixed, we cannot fit both frequency and amplitude simultaneously.

The model can now be used for analysis and controller design. This is not the focus of this paper, but it can be shown that the unstable stationary steady state can be stabilized easily using feedback control when the riser-base or a reasonably close (a few kilometers) upstream pressure can be measured. It is also possible to stabilize the flow using only upstream measurement (at or close to the choke) (10). This can be done by a combination of a flow measurement and some other measurement, e.g. pressure using a cascade controller (5). The flow can either be measured or estimated from density and pressure drop measurements.

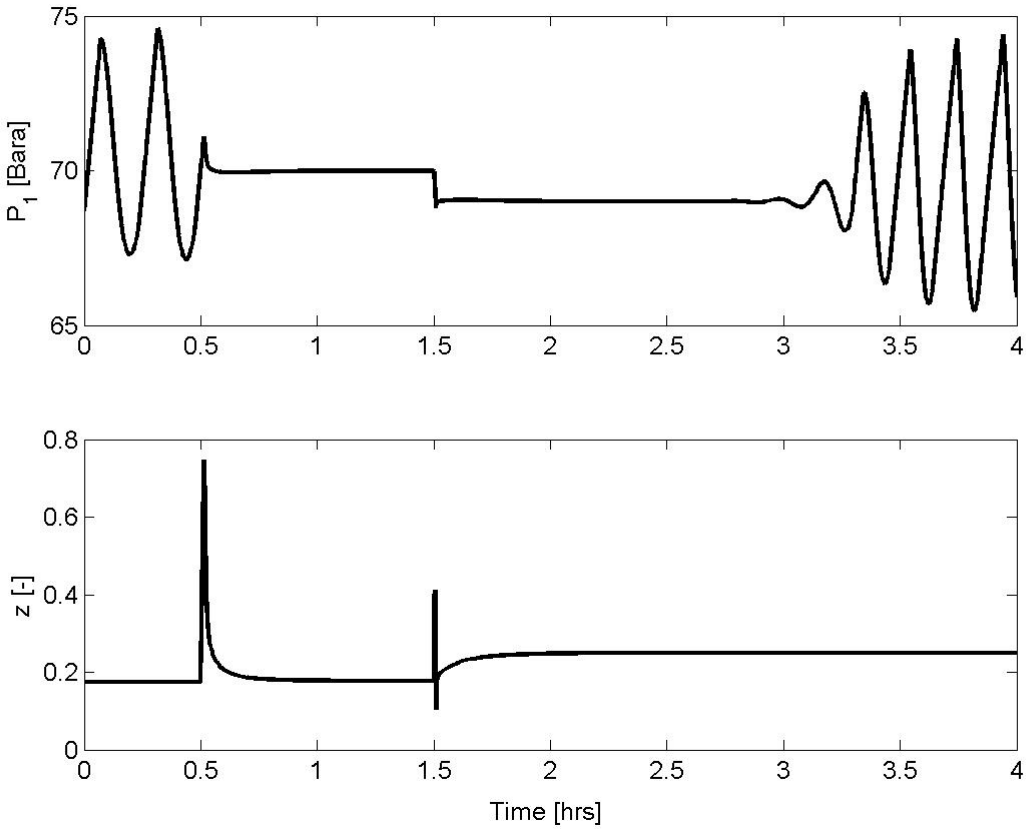

Figure 5: Stabilization of severe slugging using a PI controller with upstream pressure as measurement (Case 1)

Figure 5 shows a simulation with a PI controller designed using our simplified model stabilizing the flow. The simulations are also done using the simplified model. The top part shows the downstream pressure vs. time, the lower shows the valve position. The system is started up in open loop (controller offline) with a valve opening of z = 0.175. As predicted from the bifurcation diagram (Figure 4), severe slugging develops. The controller is turned on after 0.5 hrs, and the controller stabilizes the system rapidly at the set point of 70 Bara. After 1.5 hrs, the set point is changed to 69 Bara. The control system manages to stabilize both operating points. After 3 hours, the controller is put back in manual, leading to the reappearance of the severe slugging.

The operating point with a set point of 69 Bara corresponds to a valve opening of 0.25, which is well within the unstable region. As can be seen from Figure 5, the valve position moves towards this value, and seems to stay constant as this value. However, if one had zoomed in on the graph, or studied an actual valve used for stabilizing control, one would see that the valve is continuously making small corrections to hold the system stable. The controller designed based on the simplified model has been tested on the OLGA model with similar results.

5 CASE 2: FIT TO EXPERIMENTAL DATA

We have fitted the model to data from recent experiments performed by Statoil at a medium scale loop at the SINTEF Petroleum Research Multiphase Flow Laboratory at Tiller outside Trondheim, Norway. The loop consists of a 200 meters long slightly declining feed pipeline entering a 15 meters high vertical riser with a control valve located at the top. The fluids used are SF_6 for the gas and Exxsol D80 for the liquid. After the riser the mixture enters a gas-liquid separator with an average pressure of 2 Bara. The inflow into the feed pipeline is pressure dependent. More information on these experiments can be found in (5) and (10).

We were able to obtain a very good fit of our simplified model to the experimental results. The bifurcation chart is given in figure 6, where experimental data are given as dots. More importantly, the controllers (designed based on the simplified model) reproduced the stability results confirmed experimentally. In fact, the optimized controller tunings found using the model matched the ones found to be optimal from the experimental work.

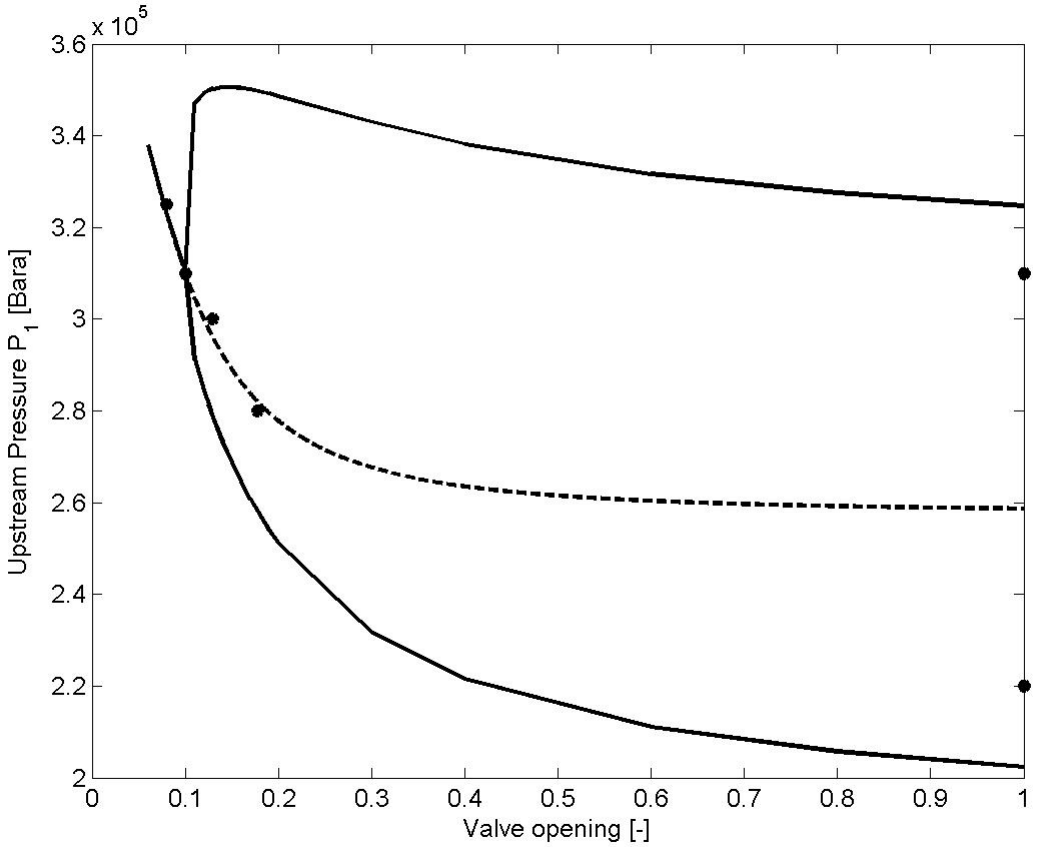

Figure 6: Bifurcation diagram for the Tiller experimental data (case 2)

6 CONCLUSIONS

We have developed a simplified model of severe slugging suitable for controller design. The model has three states and is based on "phenomenological" modeling, where we identify the major characteristics of the system at hand and develop a model that incorporates these characteristics. The major characteristics are the stability of the flow as a function of choke valve position, the nature of the transition to instability (Hopf bifurcation), the presence of an unstable steady-state solution and the amplitude of the oscillations. It should be stressed that the model, in addition to describing the (undesired) slug behavior, must describe the (desired) steady state flow regime.

Based on this model, we are able to investigate the linear and non-linear behavior of the system. We can study the nature of the instability, evaluate different measurements candidates for control and test control configurations. The model is currently used both as a tool for understanding the behavior of these systems and for designing control systems that stabilizes the flow.

We have fitted the model to data both from an OLGA test case and from medium-scale experiments. We have in both cases achieved good agreement with the data, and controllers designed based on our model are able to stabilize the flow for the systems modeled. It is also our experience that this simplified model is easier to fit to experimental data than the more

complicated PDE models that are based on a more “rigorous” representation of the true system.

We hope to test the model against field data in the near future. It is our firm belief that one can design better and more robust controllers for stabilizing multiphase flow in offshore pipeline-riser systems with less effort using a simplified model.

7 ACKNOWLEDGEMENTS

The authors would like to thank the members of the Petronics project, as well as its sponsors in Norsk Hydro and ABB. We would also like to thank Statoil for supplying experimental data and valuable insight. Finally, we would like to thank the Norwegian Research Council for financial support.

8 REFERENCES

(1) Sarica, C and Tengesdal, J. *“A new technique to eliminate severe slugging in pipeline / riser systems”*, SPE Annual Technical Conference and Exhibition 2000, Dallas, Texas. SPE63185

(2) Hende, P. and Linga, H. “*Suppression of terrain slugging with automatic and manual riser choking”*, Advances in Gas-Liquid Flows, 2000, pp. 453-469

(3) Havre, K., Stornes, K. and Stray, H. *“Taming slug flow in pipelines”,* ABB review 4, 2000, pp. 55-63

(4) Henriot, V., Courbot, A., Heintze, E. and Moyeux, L. *“Simulation of process to control severe slugging: Application to the Dunbar pipelines”*, SPE Annual Conference and Exhibition in Houston, Texas, 1999. SPE56461

(5) Skofteland, G. and Godhavn, J.M. “*Suppression of slugs in multiphase flow lines by active use of topside choke - Field experience and experimental results”*, Accepted for publication at Multiphase'03, San Remo, Italy, 11-13 June 2003.

(6) Bendiksen, K., Malnes, D. and Nydal, O.J. *“On the modeling of slug flow”*, Chemical Engineering Communications, 141: 71-103, 1996

(7) Taitel, Y. and Barnea, D. *"Two phase slug flow"*, Advances in Heat Transfer, Hartnett J.P. and Irvine Jr. T.F. ed., vol. 20, 83-132, Academic Press (1990).

(8) Storkaas, E., Alstad, V. and Skogestad, S. *“Stabilization of desired flow regimes in pipelines”*, AIChE Annual meeting 2001, Reno, Nevada. Paper 287d

(9) Matlab model available at :www.chembio.ntnu.no/users/skoge/software/index2.html

(10) Fard, M. and Godhavn, J.M. *“Modeling and Slug Control within OLGA”* Submitted to SPE Journal.

Appendix A:

The model presented below is for the case of constant inflow. For pressure dependent inflow, the model for the inflow mechanism must also be included.

A.1 Notation

Symbol	Description	Unit	Remarks
m_{Gi}	Mass of gas in volume i	kg	State variable
m_L	Mass of liquid	kg	State variable
V_{Gi}	Gas volume i	m^3	V_{G1} = const.
V_L	Volume occupies by liquid	m^3	
V_{LR}	Volume of liquid in riser	m^3	
V_T	Total volume of riser	m^3	Constant
P_i	Pressure in volume i	Pa	
ρ_{Gi}	Gas density in volume i	kg/m^3	
ρ_L	Liquid density	kg/m^3	Constant
$\overline{\rho}$	Average density in riser	kg/m^3	
ρ_T	Density at valve	kg/m^3	
v_{G1}	Gas velocity at low point	m/s	
w_{G1}	Internal mass rate of gas	kg/s	
$w_{mix,out}$	Total mass rate through valve	kg/s	
$w_{G,out}$	Mass rate of gas through valve	kg/s	
$w_{L,out}$	Mass rate of liquid through valve	kg/s	
α_L	Average liquid fraction in riser, volume basis	-	
α_{LT}	Liquid fraction at valve, volume basis	-	
α_L^m	Liquid fraction at valve, mass basis	-	
h_1	Liquid level upstream low point	m	
H_1	Critical liquid level	m	Constant
H_2	Height of riser	m	Constant
r	Radius of pipe	m	Constant
A_1	Cross section area in horizontal plane, upstream low point	m^2	Constant
A_2	Cross section area in horizontal plane, riser	m^2	Constant
$\hat{A}$	Gas flow area at low point	m^2	Constant
L_3	Length of horizontal top section	m	Constant
θ	Feed pipe inclination	rad	Constant
R	Gas constant	J/K/kmole	Const=8314
g	Specific gravity	m/s^2	Const=9.81
T	System temperature	K	Constant
M_G	Molecular weight of gas	kg/kmole	Constant
$w_{G,in}$	Mass rate of gas into system	kg/s	Disturbance
$w_{L,in}$	Mass rate of liquid into system	kg/s	Disturbance
P_0	Pressure after valve	Pa	Disturbance
z	Valve position	-	Input
K_1	Choke valve constant	-	Tuning parameter
K_2	Internal gas flow constant	-	Tuning parameter

K_3	Friction parameter	-	Tuning parameter
n	Exponent in friction expression	-	Tuning parameter

A.2 Equations

A.2.1 Internal equations

$$P_1 = \frac{m_{G1} R T}{V_{G1} M_G} \quad [14]$$

$$\rho_{G1} = \frac{m_{G1}}{V_{G1}} \quad [15]$$

$$V_L = \frac{m_L}{V_{G1}} \quad [16]$$

$$h_1 A_1 + V_{LR} = V_L \quad [17]$$

$$V_T = A_2 \left(H_2 + L_3 \right) \quad [18]$$

$$V_{G2} = V_T - V_{LR} \quad [19]$$

$$\rho_{G2} = \frac{m_{G2}}{V_{G2}} \quad [20]$$

$$\alpha_L = \frac{V_{LR}}{V_T} \quad [21]$$

$$P_2 = \frac{m_{G2} R T}{V_{G2} M_G} \quad [22]$$

$$\overline{\rho} = \frac{m_{G2} + V_{LR} \rho_L}{V_T} \quad [23]$$

$$\overline{\rho} g \left(H_2 + H_3 \right) - \rho_L g h_1 = P_1 - P_2 \quad [24]$$

$$q = \frac{K_3 \rho_{G1} v_{G1}^2}{\rho_L - \rho_{G1}} \quad [25]$$

$$\alpha_{LT} = (V_{LR} > H_2 A_2) \frac{V_{LR} - H_2 A_2}{A_3 H_3} + \frac{q^n}{1 + q^n} \left(\alpha_L - (V_{LR} > H_2 A_2) \frac{V_{LR} - H_2 A_2}{A_3 H_3} \right) \quad [26]$$

$$\rho_T = \alpha_{LT} \rho_L + \left(1 - \alpha_{LT} \right) \rho_{G2} \quad [27]$$

$$\alpha_L^m = \frac{\alpha_{LT} \rho_L}{\alpha_{LT} \rho_L + \left(1 - \alpha_{LT} \right) \rho_{G2}} \quad [28]$$

A.2.2 Transport equations

$$v_{G1} = \left(h_1 < H_1 \right) K_2 \frac{H_1 - h_1}{H_1} \sqrt{\frac{P_1 - P_2 - \rho_L g \alpha_L H_2}{\rho_{G1}}} \quad [29]$$

$$w_{G1} = v_{G1} \rho_{G1} \widehat{A} \quad [30]$$

$$w_{mix,out} = K_1 z \sqrt{\rho_T \left(P_2 - P_0 \right)} \quad [31]$$

$$w_{G,out} = \left(1 - \alpha_L^m \right) w_{mix,out} \quad [32]$$

$$w_{G,out} = \alpha_L^m w_{mix,out} \quad [33]$$

A.2.3 Geometric equations

$$H_1=\frac{2r}{\cos(\theta)}$$

$$A_1=\frac{A_2}{\sin(\theta)}$$

$$\varphi=\left((H_1-h_1)\cos(\theta)<r\right)\left(\pi-\cos^{-1}\left(1-\frac{(H_1-h_1)\cos(\theta)}{r}\right)\right)+\left((H_1-h_1)\cos(\theta)\geq r\right)\left(\cos^{-1}\left(\frac{(H_1-h_1)\cos(\theta)}{r}-1\right)\right) \quad [34]$$

$$\hat{A}=r^2\left(\pi-\varphi-\cos(\pi-\varphi)\sin(\pi-\varphi)\right) \quad [35]$$

A.2.4 Conservation equations

$$\frac{d}{dt}m_L=w_{L,in}-w_{L,out} \quad [36]$$

$$\frac{d}{dt}m_{G1}=w_{G,in}-w_{G1} \quad [37]$$

$$\frac{d}{dt}m_{G2}=w_{G1}-w_{G,out} \quad [38]$$

Appendix B: State transformation

With its current states, the model is a differential-algebraic (DAE) system. If the model is to be used for linearization or nonlinear analysis, it would be preferable to transform the system into an ODE system. This can be done through the state transformation given below.

To simplify the notation, we will scale and rename the states m_L, m_{G1} and m_{G2} to $x_1=\frac{m_L}{V_T\rho_L}$, $x_2=\frac{m_{G1}}{V_{G1}\rho_{G1}^*}$ and $x_3=\frac{m_{G2}}{V_{G2}\rho_{G2}^*}$. The quantities marked with an asterisk are reference values for the given variable. When $(\cdot)$ is used as an argument, it is an abbreviation to simplify the model and should be taken to represent the appropriate arguments for the given expression.

With the current states, the model is a DAE system. The height h_1 will be used as the algebraic state, denoted γ. Entries that are not states and that are not given with an argument are constant system parameters.

With these changes of notation, we can simplify the model to:

$$\dot{x}_1=\frac{w_{L,in}}{V_T\rho_L}-\frac{\alpha_{LT}(\cdot)\left(1-x_1+\frac{A_1}{V_T}\gamma\right)}{\alpha_{LT}(\cdot)\left(V_T-V_Tx_1+A_1\gamma\right)+V_T\rho_{G2}^*\left(1-\alpha_{LT}(\cdot)\right)x_3}\Psi(\cdot)z \quad [39]$$

$$\dot{x}_2=\frac{w_{G,in}}{V_{G1}\rho_{G1}^*}-\frac{\hat{A}(\gamma)v_{G1}(\cdot)x_2}{V_{G1}} \quad [40]$$

$$\dot{x}_3=\frac{\rho_{G1}^*\hat{A}(\gamma)v_{G1}(\cdot)x_2}{V_T\rho_{G2}^*}-\frac{\left(1-\alpha_{LT}(\cdot)\right)x_3}{\alpha_{LT}(\cdot)\rho_L\left(V_T-V_Tx_1+A_1\gamma\right)+V_T\rho_{G2}^*\left(1-\alpha_{LT}(\cdot)\right)x_3}\Psi(\cdot)z \quad [41]$$

$$\left(\rho_{G2}^{*}x_3+\rho_L x_1-\frac{\rho_L A_1}{V_T}\gamma\right)g\left(H_2+H_3\right)-\rho_L g\gamma=\frac{RT}{M_G}\left(\rho_{G1}^{*}x_2-\frac{V_T\rho_{G2}^{*}x_3}{\left(V_T-V_T x_1+A_1\gamma\right)}\right) \quad [42]$$

$v_{G1}(\cdot)$, $\Psi(\cdot)$, and $\alpha_{LT}(\cdot)$ used above is given below. $\hat{A}(\gamma)$ is given by equation 26.

$$v_{G1}(x,\gamma)=\left(\gamma<H_1\right)K_2\frac{H_1-\gamma}{H_1}\sqrt{\frac{\frac{RT}{M_G}\left(\rho_{G1}^{*}x_2-\frac{V_T\rho_{G2}^{*}x_3}{V_T-V_T x_1+A_1\gamma}\right)-\rho_L gH_2\left(x_1-\frac{A_1}{V_T}\gamma\right)}{\rho_{G1}^{*}x_2}}$$

$$\Psi\left(x,\gamma,\alpha_{LT}(\cdot)\right)=\frac{w_{mix,out}}{z}=$$

$$K_1\sqrt{\left(\alpha_{LT}(\cdot)\rho_L+\frac{V_T\rho_{G2}^{*}\left(1-\alpha_{LT}(\cdot)\right)x_3}{V_T-V_T x_1+A_1\gamma}\right)\left(\frac{V_T\rho_{G2}^{*}RTx_3}{\left(V_T-V_T x_1+A_1\gamma\right)M_G}-P_0\right)}$$

$$\alpha_{LT}\left(x,\gamma,v_{G1}(\cdot),\tilde{\alpha}_{LT}(\cdot)\right)=\tilde{\alpha}_{LT}(\cdot)+\frac{\left(K_3\rho_{G1}^{*}x_2\left(v_{G1}(\cdot)\right)^2\right)^n}{\left(\rho_L-\rho_{G1}^{*}x_2\right)^n+\left(K_3\rho_{G1}^{*}x_2\left(v_{G1}(\cdot)\right)^2\right)^n}\left(x_1-\frac{A_1}{V_T}\gamma-\tilde{\alpha}_{LT}(\cdot)\right)$$

$$\tilde{\alpha}_{LT}(x,\gamma)=\left(\left(V_T x_1-A_1\gamma\right)>H_2A_2\right)\frac{V_T x_1-A_1\gamma-A_2H_2}{A_3H_3}$$

Solving eq. 40 for x_2

$$x_2=\Phi\left(x_1,x_3,\gamma\right)=\frac{M_G g\left(H_2+H_3\right)}{RT\rho_{G1}^{*}}\left(\rho_{G2}^{*}x_3+\rho_L x_1-\frac{\rho_L A_1}{V_T}\gamma\right)-\frac{\rho_L M_G g}{RT\rho_{G1}^{*}}\gamma+\frac{V_T\rho_{G2}^{*}x_3}{\rho_{G1}^{*}\left(V_T-V_T x_1+A_1\gamma\right)} \quad [43]$$

Differentiating $\Phi\left(x_1,x_3,\gamma\right)$:

$$\frac{\delta\Phi}{\delta x_1}=\frac{M_G g\rho_L\left(H_2+H_3\right)}{RT\rho_{G1}^{*}}-\frac{V_T^2\rho_{G2}^{*}x_3}{\rho_{G1}^{*}\left(V_T-V_T x_1+A_1\gamma\right)^2} \quad [44]$$

$$\frac{\delta\Phi}{\delta x_3}=\frac{M_G g\rho_{G2}^{*}\left(H_2+H_3\right)}{RT\rho_{G1}^{*}}+\frac{V_T\rho_{G2}^{*}}{\rho_{G1}^{*}\left(V_T-V_T x_1+A_1\gamma\right)} \quad [45]$$

$$\frac{\delta\Phi}{\delta\gamma}=-\frac{M_G g\rho_L}{RT\rho_{G1}^{*}}\left(1+\frac{A_1\left(H_2+H_3\right)}{V_T}\right)+\frac{V_T A_1\rho_{G2}^{*}x_3}{\rho_{G1}^{*}\left(V_T-V_T x_1+A_1\gamma\right)^2} \quad [46]$$

A state transformation from x_2 to γ yields the new differential equation:

$$\dot{\gamma}=\frac{\dot{x}_2-\frac{\delta\Phi}{\delta x_1}\dot{x}_1-\frac{\delta\Phi}{\delta x_3}\dot{x}_3}{\frac{\delta\Phi}{\delta\gamma}} \quad [47]$$

The full expression can be found by inserting equations 39-41 and 44-46 into 47.